South East Asian J. of Mathematics and Mathematical Sciences
Vol. 19, No. 3 (2023), pp. 467-480

DOI: 10.56827/SEAJMMS.2023.1903.36 **ISSN (Online): 2582-0850**

ISSN (Print): 0972-7752

MATHEMATICAL INVESTIGATION OF OXYGEN TRANSPORT IN INTACT MUSCLES VIS-A-VIS TISSUE METABOLISM

Ahsan Ul Haq Lone and M. A. Khanday

Department of Mathematics,
University of Kashmir, Srinagar - 190006, INDIA

E-mail : ahsanulhaqlone@gmail.com

(**Received:** *Mar. 15, 2023* **Accepted:** *Dec. 10, 2023* **Published:** *Dec. 30, 2023)*

Abstract: The human muscle tissue is an active cite with varied aerobic consumption. The supply of oxygen to the muscle cells is governed by the demand for oxygen that varies across different metabolic states of the body tissues. Most of the models designed to simulate oxygen flow in the body are based on the assumption of constant rate of oxygen consumption in muscle tissues. This generates a picture contrary to the physiological ambience where the rates vary in response to level of activity in which muscles are involved. In this context, we have taken recourse to a comparative analysis of zero-order, first-order and Michaelis-Menten oxygen consumption rate inside the muscle tissue. The model is based on the reaction-diffusion equation, and the exact solution is obtained and compared with the numerical solution using MATLAB and both are in good agreement.

Keywords and Phrases: Oxygen tension, Oxygen consumption, Finite difference method.

2020 Mathematics Subject Classification: 92-XX, 92BXX, 92B05.

1. Introduction

Our aim in this paper is to focus on the delivery of oxygen into one of the most metabolically active tissues of the human body, i.e., the skeletal muscle. The existing models available in the literature [12, 16, 18] for oxygen transport and consumption in muscle tissues are more theoretical and lack synchrony with the real physiological conditions. Also, the models are usually reliant upon constant

consumption of oxygen in the muscle tissue that is unusual and unrealistic for muscle cells in a human body [6, 10]. The cells constituting the muscles in a human body are rather more active than any other tissue with wide-ranging levels of oxygen consumption. The varied metabolic rates demand for varied oxygen supply commensurate with varied consumption levels. The oxygen is brought to muscle cells by innervating capillaries from where its entry into muscle cells is governed by the diffusion [4, 17]. The oxygen supply to muscle cells is based on the respiratory demands that vary from one metabolic state of the body to another. The human body is constantly involved in performing metabolic functions, even at rest (basal metabolism) that necessitates the continuous supply of energy to the tissues [14, 15]. Skeletal muscles are regularly involved in various energy-demanding activities so much so that the skeletal tissues are the most active consumers of oxygen in human body. During exercise or active manual works, skeletal muscles are actively involved in respiration, with oxygen consumption occurring at an accelerated rate. The high demands of oxygen consumption in an exercising muscle are met by increase in the coordinated activity of lungs and heart that makes oxygen available to actively respiring tissues. Key studies have been undertaken by various researchers that reveal an enzymatic regulation of oxygen in muscle cells [3]. However, continued exercise may push oxygen consumption beyond threshold level and lead to depletion in oxygen concentration in the skeletal tissue that is finally translated into switch-over to anaerobic mode of respiration. As a result, lactic acid accumulates in muscle cells, leading to exhaustion and muscle cramps.

The main objective of this paper is to understand the delivery of oxygen into muscles tissue that is driven by the diffusion of oxygen from capillaries into skeletal cells. The diffusion gradient changes in response to change in the partial pressure of oxygen across the two ends of the diffusion pathway-capillary end and tissue end. One of the most important factors responsible for change in the partial pressure of oxygen and hence, the diffusion, is the rate of its consumption in the skeletal tissue. Earlier studies on modelling of oxygen delivery into the tissue have modelled oxygen consumption using zero-order oxygen consumption rate, instead of first-order and Michaelis-Menten oxygen consumption rate, as a presumption for the development of the model [9, 13]. Using zero-order oxygen consumption rate approach, oxygen consumption is a positive constant where oxygen concentration is greater than zero, and oxygen consumption is zero where oxygen concentration is zero. However, the metabolic condition of tissues changes with the change in activity of the human body and hence, there is change in the rate of oxygen consumption in the corresponding tissue.

Human skeletal tissue shows least metabolic activity at rest, the state of low

oxygen consumption. However, the increase in the activity of muscles (e.g., in exercise) increases the metabolic rate and oxygen consumption in muscle cells. In this backdrop, for the development of a more realistic model, it is imperative to consider varying rates of oxygen consumption in tissues. The present approach is intended to build upon already existing models [6] and to devise a more realistic model by taking into account varying rates of oxygen consumption in the skeletal tissue across different metabolic states of the human body, from rest to rigorous exercises. In this paper, we formulate a mathematical model of oxygen transport in intact muscle vis-a-vis tissue metabolism. The model is based on the reaction-diffusion equation and has been solved for zero-order and first-order oxygen consumption rate analytically in steady state case, and numerically in unsteady state case. In addition, we have taken recourse to Michaelis-Menten oxygen consumption rate that accounts a non-linear transport and consumption of oxygen in skeletal tissues, in an attempt to bring it in line with the actual physiological conditions.

2. Formulation of the Model

Table 1: Nomenclature and numerical values of different physiological parameters used in the model are described with units [4, 12, 17].

Parameter	Value	Unit
D,Oxygen diffusion coefficient	2.41×10^{-5}	cm^2/sec
σ, Oxygen solubility coefficient	3.89×10^{-5}	$ml\ O_2/ml/mmHg$
P^*, Average capillary partial pressure of oxygen	48	$mmHg$
k, Mass-transfer coefficient	30	$mmHg/sec$

Oxygen diffusion in tissue is governed by the reaction-diffusion equation:

$$\frac{\partial P}{\partial t} = D\frac{\partial^2 P}{\partial x^2} - \frac{1}{\sigma}M(P) + k\Big(1 - \frac{P}{P^*}\Big) \tag{1}$$

In Equation (1), three effects are included that can change the tissue partial pressure of oxygen P at a given time t. The first term in Equation (1), given by $D\frac{\partial^2 P}{\partial x^2}$, is diffusion of O_2 which occurs in living tissue due to O_2 gradients and can serve to increase or decrease partial pressure P. Oxygen diffusion would normally occur in all three spatial directions; however, variations in y and z are not included in the model. The second effect included in Equation (1), given by $M(P)$, is the oxygen uptake function, which we emphasise is a function of P. The third effect

included in Equation (1), given by $k\left(1-\frac{P}{P^*}\right)$, is blood-tissue oxygen transfer. The parameter k is used to represent the average flux of oxygen for a given difference between tissue, P, and capillary, P^*, partial pressure of oxygen values.

We consider three models of oxygen consumption that are used to describe $M(P)$ and are discussed below:

2.1. Zero-order Oxygen Consumption Model

For zero-order oxygen consumption rate (constant uptake), we have

$$M(P)=\begin{cases} M_0=\text{constant} & \text{for} \quad P>P_{cric} \\ 0 & \text{for} \quad P\leq P_{cric} \end{cases} \tag{2}$$

where M_0 is the oxygen demand and P_{cric} is the critical oxygen tension level. For numerical computation, the value of M_0 is taken as $M_0=1.50\times10^{-4}ml\ O_2/ml/s$.

Therefore, model Equation (1) can be written as

$$\frac{\partial P}{\partial t}=D\frac{\partial^2 P}{\partial x^2}-\frac{1}{\sigma}M_0+k\left(1-\frac{P}{P^*}\right)=D\frac{\partial^2 P}{\partial x^2}+A_0-B_0P \tag{3}$$

2.2. First-order Oxygen Consumption Model

For first-order oxygen consumption rate (linear uptake), we have

$$M(P)=\alpha P \tag{4}$$

where α is the maximum reaction rate.

Therefore, model Equation (1) becomes

$$\frac{\partial P}{\partial t}=D\frac{\partial^2 P}{\partial x^2}-\frac{\alpha P}{\sigma}+k\left(1-\frac{P}{P^*}\right)=D\frac{\partial^2 P}{\partial x^2}+A_1-B_1P \tag{5}$$

2.3. Michaelis-Menten Oxygen Consumption Model

For Michaelis-Menten oxygen consumption rate (non-linear uptake), we have

$$M(P)=M_0\frac{P}{P+P_m} \tag{6}$$

where P_m is the value of P at which the rate of reaction is half-maximal.

Therefore, model Equation (1) becomes

$$\frac{\partial P}{\partial t}=D\frac{\partial^2 P}{\partial x^2}-\frac{M_0}{\sigma}\frac{P}{P+P_m}+k\left(1-\frac{P}{P^*}\right) \tag{7}$$

where $A_0 = k - \dfrac{M_0}{\sigma}$, $B_0 = \dfrac{k}{P^*}$, $A_1 = k$ and $B_1 = \dfrac{k}{P^*} + \dfrac{\alpha}{\sigma}$. When $P_m \to 0$, the Michaelis-Menten oxygen consumption rate model approaches to zero-order oxygen consumption rate model, $M \to M_0$. For small values of oxygen tension, $P << P_m$, the Michaelis-Menten oxygen consumption rate model approaches to first-order oxygen consumption rate model.

3. Solution of the Models

The governing Equations (3) and (5) shows that, in addition to D, there are two constants (assumed to be positive) that determine the dynamics of P; A_0 (A_1)-which represents the balance between capillary O_2 supply and tissue O_2 consumption when $P = 0$ (maximum O_2 flux into the tissue); and B_0 (B_1)-which determines how O_2 flux into the tissue decreases for $P > 0$.

Model Equations (3) and (5) are linear one-dimensional reaction-diffusion equations. For appropriate initial and boundary values, it will have unique bounded and continuous solution. For steady-state conditions, we use boundary conditions for $x \geq 0$ and $t \geq 0$ that represent partial pressure of oxygen fixed at the surface P_s of the muscle ($x = 0$):

$$P(x = 0) = P_s, \quad \text{and} \quad P(x \to \infty) < \infty \tag{8}$$

where the second boundary condition is required to eliminate the exponentially growing solution (e^{bx}), which would lead to an unrealistic outcome result (infinite P) as $x \to \infty$. Integration of the steady-state form of the partial differential Equations (3) and (5) then yields the solutions, respectively:

$$P_{steady} = \frac{A_0}{B_0} + \Big(P_s - \frac{A_0}{B_0}\Big)e^{-bx}, \quad \text{and} \quad P_{steady} = \frac{A_1}{B_1} + \Big(P_s - \frac{A_1}{B_1}\Big)e^{-bx} \tag{9}$$

The constant $b = \sqrt{\dfrac{B_0}{D}}$ represents the rate at which the tissue partial pressure of oxygen changes from the value set at the surface (P_s) to its natural far-field value $\Big(P(x \to \infty) = \dfrac{A_i}{B_i},\ i = 0, 1\Big)$. As the diffusion coefficient D increases, b becomes smaller because the influence of the surface partial pressure of oxygen extends further into the tissue. On the other hand, as the constant B_0 increases, b becomes larger because the effect of capillary O_2 delivery to the tissue becomes stronger.

The initial condition associated with the model Equation (1) is:

$$P(x, 0) = u_0 + \Big(P_s - u_0\Big)e^{-bx} \tag{10}$$

where u_0 is constant partial pressure of oxygen far from the capillary surface.

The exact solution of the model Equation (7) is very difficult to process due to the involvement of non-linear Michaelis-Menten oxygen uptake function (6). So, a finite-difference method has been used to solve the models.

3.1. Finite-Difference Method

The analytic solution to the model Equation (1) gives the oxygen partial pressure $P(x,t)$ as a continuous function of x and t that can be evaluated at any point in the muscle tissue domain. Let's cover muscle tissue by a uniform mesh (or grid) as shown in Figure 1 where the grid points are $(x_j = j\triangle x, t_n = n\triangle t)$, $\triangle x = h$ and $\triangle t = k$ are the step sizes in the $x-$ and $t-$directions, respectively. Each node in the grid is identified by an ordered pair of integers (j,n). A finite-difference method aims at determining numerical values for P at the discrete set of points specified by the grid (x_j,t_n), that is to determine $P(x_j,t_n) \equiv P_j^n$ for all values of j and n in the grid ($j-$space step parameter and $n-$time step parameter). Afterward, suitable interpolations can be used to find P at intermediate points not specified by the grid, if desired.

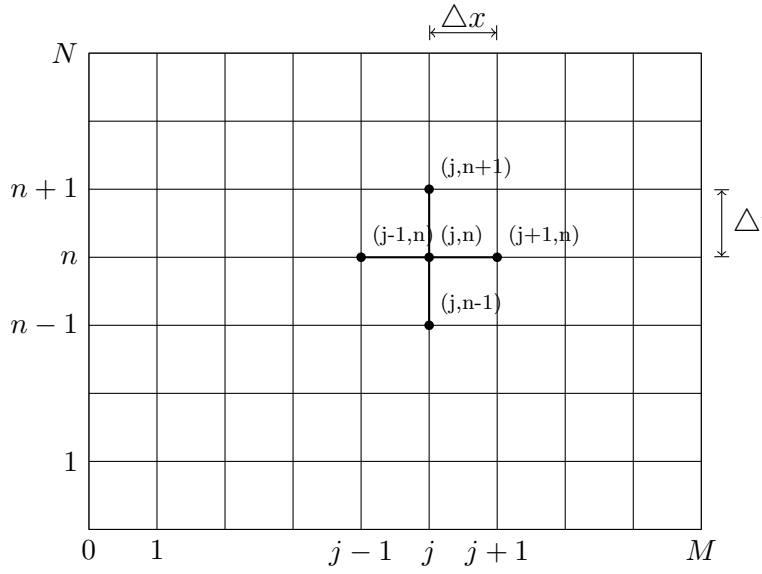

Figure 1: Mesh showing discretization of time and space domain.

Definition 1. *A finite-difference approximation to the second-order partial deriva-*

tive of $P(x,t)$ with respect to space variable x defined by, where $\theta \in [0,1]$,

$$\frac{\partial^2 P}{\partial x^2} = \theta \frac{P_{j+1}^{n+1} - 2P_j^{n+1} + P_{j-1}^{n+1}}{h^2} + (1-\theta)\frac{P_{j+1}^n - 2P_j^n + P_{j-1}^n}{h^2} \tag{11}$$

is known as θ-method (theta-method) [8].

Consider model Equation (1) subjected to the initial condition (10) and boundary conditions (8). The muscle tissue region $\Omega = [0,L] \times [0,T]$ is discretized by the uniformly distributed grid points (x_j, t_n), where

$$\begin{aligned} x_j &= jh, \quad j = 0,1,2,\cdots,M, \quad Mh = L \\ t_n &= nk, \quad n = 0,1,2,\cdots,N, \quad Nk = T; \quad M, N \in \mathbb{Z}_{\geq 0} \end{aligned}$$

Moreover, P_j^n denotes the mesh (or grid) function that approximates $P(x_j, t_n)$ for $j = 0,1,2,\cdots,M$ and $n = 0,1,2,\cdots,N$. Therefore, model Equation (1) is approximated by the following finite difference equations [7]:

$$\begin{aligned} \frac{P_j^{n+1} - P_j^n}{k} &= D\theta \frac{P_{j+1}^{n+1} - 2P_j^{n+1} + P_{j-1}^{n+1}}{h^2} + D(1-\theta)\frac{P_{j+1}^n - 2P_j^n + P_{j-1}^n}{h^2} \\ &\quad - \frac{MP_j^n}{\sigma} + k\Big(1 - \frac{P_j^n}{P^*}\Big) \end{aligned}$$

where θ, $0 \leq \theta \leq 1$, is the weight of the function. Depending on the values of θ, we get forward-time central-space (FTCS) method (Schmidth method) if $\theta = 0$, backward-time central-space (BTCS) method (Laasonen method) if $\theta = 1$ and Crank-Nicolson Scheme if $\theta = \dfrac{1}{2}$.

By using forward-time central-space (FTCS) method over the domain $\Omega = [0,L] \times [0,T]$, we obtain the values of P at the nodal points with respect to the following uptake functions:

- For constant uptake function, we have

$$P_j^{n+1} = a_1 P_{j+1}^n + (1 - 2a_1 - B_0)P_j^n + a_1 P_{j-1}^n + A_0 \tag{12}$$

- For linear uptake function, we have

$$P_j^{n+1} = a_1 P_{j+1}^n + (1 - 2a_1 - B_1)P_j^n + a_1 P_{j-1}^n + A_1 \tag{13}$$

- For Michaelis-Menten uptake function, we have

$$P_j^{n+1} = P_{j+1}^n + (1 - 2a_1 - B_0)P_j^n + a_1 P_{j-1}^n + A_1 - b_1 \frac{P_j^n}{P_m + P_j^n} \tag{14}$$

where $a_1 = \dfrac{D\triangle t}{\triangle x^2}$, $b_1 = \alpha\triangle t$, P_j^n is a grid function on the grid points $x_j = j\triangle x,\ j = 0, 1, 2, ..., M$ and $t_n = n\triangle t,\ n = 0, 1, 2, ..., N$, and M and N are, respectively, the number of subdivisions in the axial and time directions of the discretized tissue region.

The initial condition (10) takes the form: $P_j^0 = u_0 + \Big(\ P_s - u_0\Big)e^{-j\triangle x.b}$ and the boundary conditions become: $P_0^n = P_s, \quad$ and $\quad P_M^n = u_0$. The numerical method used is consistent as discussed in Lone et al. [6] and stable by the following criteria [1, 11]:

$$1 - 2a_1 - B_0 \geq 0 \quad \text{or} \quad 1 - 2a_1 - B_1 \geq 0 \quad \text{or} \quad 1 - 2a_1 - B_0 \geq 0 \quad \text{as} \quad B_0 < B_1$$
$$\Rightarrow \quad \frac{\triangle t}{\triangle x^2} \leq \frac{1 - B_0}{2D}$$

For finite values of $\triangle x$ and $\triangle t$, the finite-difference solution P_j^n is not identical to the exact solution $P(x_j, t_n)$. The solution error or simply error is $SE = |e_{j,n}| = |P_j^n - P(x_j, t_n)|$. The L2-norm is used to assess the error between the numerical solution P_j^n and the analytical solution $P(x_j, t_n)$ [5]:

$$\big|\big|e\big|\big|_2 = \left(\frac{1}{MN}\sum_{i=1}^{M}\sum_{j=1}^{N}\big|e_{j,n}\big|^2\right)^{1/2} = \left(\frac{1}{MN}\sum_{i=1}^{M}\sum_{j=1}^{N}\big|P_j^n - P(x_j, t_n)\big|^2\right)^{1/2} \tag{15}$$

where the numerical approximation, P_j^n, is a grid function on the grid points. The boundary condition and the initial condition are not included in this error estimate, because these values are specified and not approximated. The error estimate (15) is analogous to the root-mean-square error defined as the square root of the mean of the errors between measured values and values predicted by a model.

For all computational work, MATLAB software has been used for analysis.

4. Results and Discussion

In this paper, oxygen transport model equations are presented in an attempt to bring them in line with the real physiological conditions. The formulated models in the form of oxygen uptake functions take into account all possible conditions ranging from constant consumption (indicative basal metabolism in the body) to varied or oscillating rates (connecting work activities of varied magnitudes) of oxygen consumption in the muscle tissues. The results presented in the form of graphs using MATLAB are more or less in consonance with known physiological ambience. Our models are based on the presumption of non-uniform blood flow denoted by

different values of mass-transfer coefficient k, which is in effect determined by variation in oxygen demand by muscle cells. The numerical values of the parameters taken for the computation are given in Table 1.

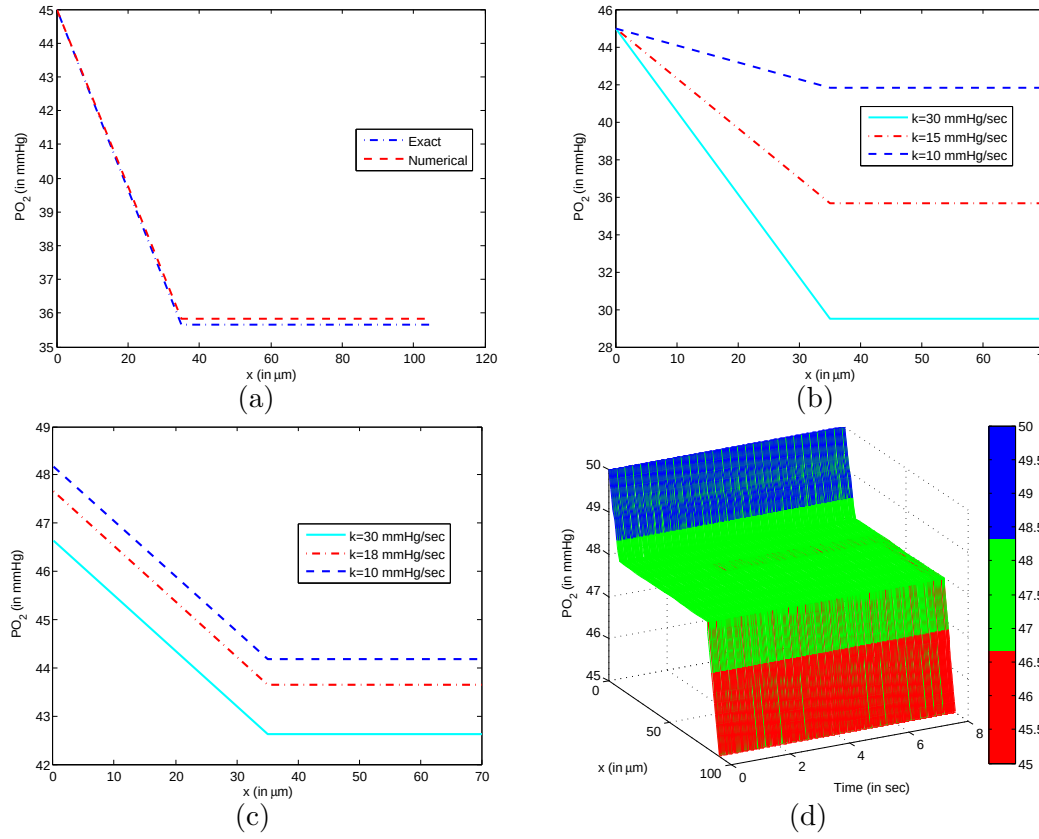

Figure 2: (a) Comparison of oxygen concentration in the tissue compartment, (b) Temporal variation of pulmonary administration of oxygen concentration in the arterial blood compartment, (c) Temporal variation of intravenous administration of oxygen concentration in the arterial blood compartment, (d) Temporal variation of intravenous administration of oxygen concentration in the Tissue compartment at rates $/sec : (i) = \{a_{31} = 1.98,\ a_{12} = 1.32\},\ (ii) = \{a_{31} = 1.5,\ a_{12} = 1.0\},\ (iii) = \{a_{31} = 0.975,\ a_{12} = 0.625\}$ and $(iv) = \{a_{31} = 0.4,\ a_{12} = 0.27\}$ with $p_0 = q_0 = 5 \times 10^{-6}\ mol\ cm^{-3}$.

Numerical method has been used to solve the model that is based on the finite difference method known as forward-time central-space (FTCS) method. We have computed the exact solution and compared with FTCS solution for validation of the result and found that there is a good agreement between both which is shown in Figure 3a.

The first model lays out the zero-order oxygen consumption rate inside the muscle tissue. A comparison is made between P across spatial dimensions of muscle tissue with respect to different mass-transfer coefficients k of oxygen taken at 10 $mmHg/sec$, 15 $mmHg/sec$ and 30 $mmHg/sec$, as shown in Figure 2b. It is a steady state simulation of oxygen consumption inside the muscle tissue. Regardless of the values of k, the results show an initial decrease in P up to some level where from the value of P inside muscle tissue remains same. The results are indicative of a constant metabolic rate inside the muscle cells that is reflected in the constant consumption of oxygen inside the cells after achieving a fixed level in the beginning. The effect of k is reflected in a significant divergent shift of the curves and the degree of steepness associated therewith.

The second model represents the oxygen consumption inside the muscle tissue with respect to first-order oxygen consumption rate. For different values of mass-transfer coefficient k (10 $mmHg/sec$ *vs.* 30 $mmHg/sec$), the model predicts parallel response of P with an initially decreasing trend followed by an indefinite constancy after reaching certain distance along the axis of oxygen transfer pathway (Figure 2c). The model is again based on steady state assumption, i.e., the oxygen consumption rate is viewed independent of time.

In Figure 2d, an analysis of the models is presented in a three-dimensional form in order to present a broader picture of the proposed models.

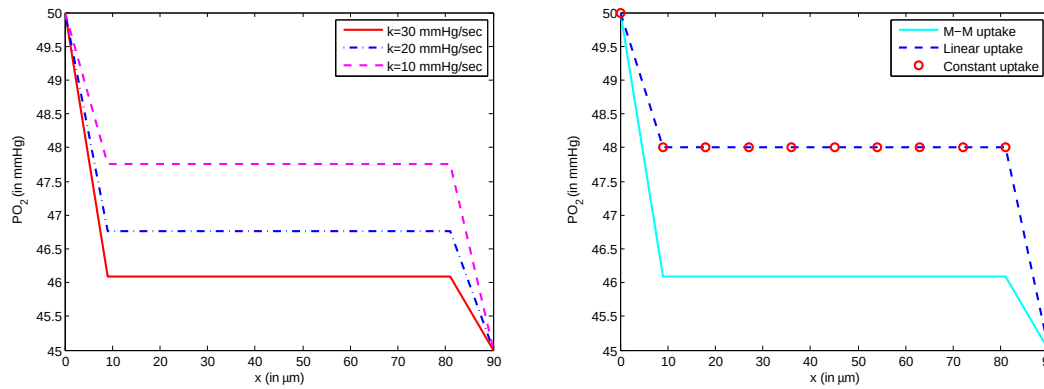

Figure 3: (a) Tissue oxygen tension profiles for Michaelis-Menten oxygen consumption rate and $t = 20$ sec, (b) Tissue oxygen tension profiles for zero-order, first-order and Michaelis-Menten oxygen consumption rate ($k = 20$ $mmHg/sec$ and $t = 20$ sec). The solid line ($-$) represents the simulation with the Michaelis-Menten uptake function given by the Equation (6), the dashed line ($--$) represents the simulation with the linear uptake function given by Equation (4), and the circles ($\circ\ \circ$) represents the simulation with the constant uptake function given by Equation (2).

The third model proposed in this paper is based on Michaelis-Menten oxygen consumption rate. This model is introduced to account for multi-dimensional analysis of problem at hand. The cellular demands for oxygen and the rate of oxygen consumption do not remain constant in physiological circumstances of muscle; rather, the rate of oxygen supply and consumption change with time in relation to the level of activity in which the tissue is involved. Michaelis-Menten oxygen consumption rate is applied to predict oxygen uptake in muscle tissues in terms of change in partial pressure of oxygen. Figure 3a yields different patterns of oxygen uptake (presented in the form of P) across different values of mass-transfer coefficient, k. Higher values of mass-transfer coefficient k, yielded correspondingly higher levels of oxygen uptake shown as drop in the level of partial pressure of oxygen in the tissues. The results are in agreement with ambient physiological parameters where high muscular activity is met with increased blood supply and higher consumption in respiratory metabolism.

Oxygen consumption is not constant in biological systems. To examine whether the proposed model sufficiently predicts this distinction, cross-comparison of zero-order, first-order and Michaelis-Menten oxygen consumption rate inside the muscle tissue was made while taking a fixed point of time, as shown in Figure 3b. The zero-order and first-order oxygen consumption rate models show coincidence of trajectories with relatively less uptake of oxygen. This ascertains the oxygen consumption during the time of least metabolic activity of muscle cells (basal metabolism). The difference is seen in Michaelis-Menten oxygen consumption rate model, where oxygen consumption is high, commensurate with increased metabolic activity of muscle cells. It is pertinent to mention that in steady state models the results display only an initial decrease in P, whereas in unsteady state models the decrease in P recurs after attaining a constant value.

5. Conclusion

In conclusion, it appears that our model is able to predict the behaviour of muscles vis-a-vis demand of oxygen and its consumption rate in varied activities of human body. The proposed models may specifically find application in sports and athletics, where muscular tissues are vigorously involved. This work can be further extended by adding variations along y and z-directions, variable diffusivity and other environmental issues as parameters into the model.

Acknowledgements

This work was supported by the SERB-DST, Government of India, under award No.-EMR/2015/002487.

References

[1] Crank J., The Mathematics of Diffusion, Oxford, 2nd ed., 1975.

[2] Crank J. and Gupta R. S., A moving boundary problem arising from the diffusion of oxygen in absorbing tissue, J. Inst. Maths. Applics., 10 (1972), 19-33.

[3] Farmery A. D. and Whiteley J. P., A mathematical model of electron transfer within the mitochondrial respiratory cytochromes, J. Theor. Biol., 213 (2001), 197-207.

[4] Guyton A. C., Hall J. E., Text Book of Medical Physiology, W. B. Saunders, 12th ed., 2011.

[5] LeVeque R. J., Finite difference methods for ordinary and partial differential equations: steady-state and time-dependent problems. Philadelphia: SIAM (2007).

[6] Lone A. U. H., Khanday M. A., Saqib Mubark, Explicit finite difference method to estimate oxygen concentration in biological tissues under variable oxygen tension in capillaries, Comp and Math Methods, 3(2) (2021).

[7] Martin-Vaqueroa J., Sajavicius S., The two-level finite difference schemes for the heat equation with nonlocal initial condition, Applied Mathematics and Computation, 342 (2019), 166-177.

[8] Modanli M., Akgul A., Numerical solution of fractional telegraph differential equations by theta-method, Eur. Phys. J. Special Topics, 226 (2017), 3693-3703.

[9] Murray J. D., On the role of myoglobin in muscle respiration, J. Theor. Biol., 47 (1974), 115-126.

[10] Murray J. D., On the molecular mechanism of facilitated oxygen diffusion by haemoglobin and myoglobin, Proc. Roy. Soc. Lond. B. 178 (1971), 95-110.

[11] Nian li, Joseph Steiner, Shimin Tang, Convergence and stability analysis of an explicit finite difference method for 2-dimensional reaction-diffusion equations, Austral. Math. Soc. Ser., B 36, 234-241.

[12] Popel A. S., Theory of oxygen transport to tissue. Critical reviews in biomedical engineering, 17 (1989), 257-321.

[13] Salathe E. P. and Kolkka R. W., Reduction of anoxia through myoglobin-facilitated diffusion of oxygen, Biophys. J., 50 (1986), 885-894.

[14] Schumacker P. T., Chandel N., Agusti A. G. N., Oxygen conformance of cellular respiration in hepatocrytes, Am. J. Physiol., 265 (1993), L395-L402.

[15] Sim J., Cowburn A. S., Palazon A., ..., Johnson R. S., The factor inhibiting HIF asparaginyl hydroxylase regulates oxidative metabolism and accelerates metabolic adaptation to hypoxia, Cell Metabolism, 27 (2018), 898-913.

[16] Taylor B. A. and Murray J. D., Effect of rate of oxygen consumption on muscle respiration, J. Math. Biol., 4 (1977), 1-20.

[17] Tortora G. J., Derrickson B., Principles of Anattomy and Physiology, John Wiley & Sons, Inc., 13th ed., 2012.

[18] Whiteley J. P., Gavaghan D. J. and Hahn C. E. W., Mathematical modelling of oxygen transport to tissue, J. Math. Biol., 44 (2002), 503-522.